EVS38
Göteborg, Sweden, June 15-18, 2025

Optimizing Electric Vehicle Power Nets: A Data-Driven Approach to Zonal LV Architecture

Sebastian Jagfeld[1,2,*], Richard Weldle[1], Tobias Schlautmann[1], Alexander Fill[2], Kai Peter Birke[2]

[1] *Schaeffler AG*

[2] *Institute for Photovoltaics, Chair of Electrical Energy Storage Systems*

[*] *Sebastian.Jagfeld@vitesco.com*

Executive Summary:

This study addresses the challenges of increasing complexity in low-voltage (LV) power nets in battery electric vehicles (BEVs) by investigating zonal LV power supply architectures. Through measurements in three EVs, including the wiring harness, load profiles, and capacities, an extensive database of LV components was created. This database, enriched with 3D spatial data, enables analyses such as 2D load mapping and the design of a potential zonal architectures. A tool was developed to facilitate the design of zonal power supply architectures, allowing for a profound analysis of power requirements, load distribution, and potential wire length reductions. This data-based approach enables early analysis and evaluation of potential zone architectures.

1 Introduction

In 2024, Volkswagen AG announced a partnership with Rivian for the development of its future E/E architecture. According to press reports, Volkswagen wants to catch up on its software backlog and drive forward the area of software-defined vehicles [1]. Software-defined vehicles require specific hardware such as Zone Controllers (ZCs). According to Volkswagen, they already have a demonstrator car using Rivian's ZCs built up and running [2], [3]. Rivian, in turn, introduced their Gen2 E/E architecture, which is based on three in-house designed ZCs which also include power distribution and only four additional Electric Control Units (ECUs) instead of 23 main ECUs and fuse boxes in their Gen1 vehicles [4]. Tesla significantly reduced the number of electronic control units (ECUs) and fuse boxes with the Model 3 in 2017 by introducing electronic fuses (electronic fuses) and combining ECUs with power distribution into new zone controllers [5]. Most other cars on the market still rely on distributed or domain-based E/E architecture with multiple function-specific ECUs and centralized tree-shaped power distribution using melt fuse boxes. Due to the improvement potential of a zonal architecture, other OEMs are likely to follow suit. In zonal architectures, the LV power net is divided into distinct zones, each managed by a dedicated ZC. The ZC can combine the control function of ECUs with the power distribution function of fuse boxes by using electronic fuse [6]. McKinsey predicts the share of zonal architectures to be 20 % in 2030 and a continuously decreasing market

for conventional ECUs, whereas the overall automotive compute unit market will strongly increase [7].

The trend of the implementation of zonal architectures is challenging for the automotive supplier industry. Today, a large number of companies develop and produce various ECUs for the automotive industry and thus profit from the large market. Some only produce selected function-specific ECUs, while others have a wide range of knowledge and ECUs that they can cover. The supplier must possess extensive knowledge of the individual ECUs' functionality, which is reflected in the specific hardware requirements.

With the introduction of zonal E/E architectures, the ECU-market will change. Simply understanding specific ECUs won't be enough. Only the companies understanding the overall system and the individual ECU functions will succeed on the zonal controller market.

As mentioned above, ZCs combine the control function with the power distribution function of fuse boxes. Therefore, a zonal architecture also strongly impacts the power supply net. In addition to the introduction of SDV, the simplification of the wiring harness is one of the main reasons for the introduction of a zonal architecture and will therefore change significantly. By now, the wiring harness is one of the most expensive parts for a carmaker to buy. The ZCs allow the overall wiring harness to be divided into smaller, more standardized pieces, which are simpler to manufacture and assemble in the car [8]. Rivian states that it has reduced its amount of wires and thus could reduce the overall vehicle weight by about 20 kg by implementing their Gen2 ZC based electronics [4]. BMW states that its zonal wiring harness in the "Neue Klasse" shows a weight reduction of 30 % and a variant reduction by a factor of 3000, which will allow automated production in the future [9]. Other research is done on the impact of zonal architecture on the wiring harness: Park et al. prognose a reduction in the communication wiring harness length to about 50 % of its original length when implementing a six-zone architecture in comparison to a domain architecture [10]. Jang et al. see a reduction of 21 % of wire length when implementing a hybrid zonal architecture in comparison to a domain architecture [11]. Maier et al prognose an impact on the wiring harness weight, but nearly no reduction of the wiring harness length [12].

The new zone controllers and their requirements are heavily influenced by the components they need to supply. The number and type of loads to be supplied strongly influences the number and type of electronic fuse required. Existing research primarily focuses on the communication part of the zonal architecture and the wiring harness [10], [11], [13]. For the effective design and optimization of zonal architectures, detailed knowledge and real-world measurements of existing LV power nets and their components are necessary. This study presents a hands-on approach, where the physical properties of the LV power nets in three different BEVs was measured and the data used to develop a empirical tool to support the design of a zonal architecture and its power supply components.

2 Methodology

In the following section it is explains, how the data-driven approach for the zonal-architecture tool is realized. Section 2.1 describes the conducted measurements and Section 2.2 how this data is used in the zonal architecture tool.

2.1. Vehicle Analysis

As a base for the tool, vehicle data is required. Two types of studies were performed: Virtual vehicle analyses were conducted to gain 3D data on the wiring harness. Vehicle measurements were performed, focusing on the loads within the same three test vehicles. The three vehicles from the B-, C-, and J-segments cover a wide range from basic to luxurious equipment levels. The used virtual vehicle database contains 3D models of various vehicles that can be virtually dismantled [14]. This made it possible to localize all LV loads and power distribution boxes. For each load, a 3D vector tracing the supply wire was created. The 3D wiring harness data was enriched with additional information, including the supply point (fuse box), the connected load, used wire cross-sections, and fuse protection details, resulting in a detailed characterization of each load and its supply line in an extensive Matlab database. More physical properties and analytical parameters, such as, wire resistances, inductances, and a wire length factor, were also calculated and added into the data set. Here, the wire length factor describes the ratio between the actual length of the wire as it was determined in the virtual harness analysis and the geometric distance between the load and its supplying distribution box. This factor can be used to estimate the length of new supply lines, which is particularly useful for the zonal architecture tool, where loads will be reconnected to newly introduced power distribution points.

Additionally, the current profiles of the LV-loads connected to the fuse boxes were recorded for each of the

three vehicles. The load data is important for dimensioning potential ZCs and for calculating the overall power requirement, as well as studying occurring voltage drops over the wiring harness. Since the LV-system is typically concealed, distribution boxes (fuse boxes and body domain controllers) with melting fuses were used as access points for the conducted in-vehicle measurements. Special adapters, which replaced the individual melting fuses, allowed the integration of the required measurement equipment. Using this setup, each fuse was replaced, and the corresponding loads were then activated individually one after the other. All load currents were recorded in estimated maximum power conditions, such as heaters at maximum level or steering in a stationary position on a high-friction surface. Based on the recorded load profiles, the following values were determined for each measurement: maximum current (I_{max}), mean current (I_{mean}), and maximum constant current ($I_{max,const}$), with the latter representing the highest continuous current observed during the measurement, excluding transient peaks such as those caused by DC motor startups. This value indicates a maximum power condition that may persist for an extended period (multiple seconds) and is not reflected in the average current.

In addition, the input capacities of the LV loads connected to the power network were determined. The capacitance is important as it influences voltage and current dynamic and generates oscillations in the power net during switch-on which must be controlled by the ZCs. Direct measurement using an LCR meter was found to be impractical and imprecise. Instead, a similar method as described in [15] was used. For this purpose, the melting fuse for each load was disconnected to cut off the voltage supply. The remaining charge of the input capacitor of the load was then discharged via a resistor to 0 V. Subsequently, the load was recharged to the battery voltage level, and the inrush current was measured. By integrating the charge current and then dividing by the battery voltage, the capacities could be calculated. The measurement results for each load were added to the data set, ensuring that for each LV load in the system, the position, wire parameters and routing, current profile, and capacity are known. Further details on the measurement campaign can be found in [16].

2.2 Zonal Architecture Evaluation Tool

The compiled database for three evaluated vehicles facilitated the development of a tool to analyze the impact of the segmentation of the vehicle into supply zones in varying configurations. The tool enables the division of each vehicle into a variable number of zones, with each load assigned to one zone based on its geometric position. The new wire lengths for all loads are estimated using a previously determined wire length factor and the geometric distance from the load to its corresponding ZC. Special requirements, such as the crossed supply of low beam and high beam, are ignored for these considerations. So the tool enables an evaluation of the effects of the selected segmentation in a zonal architecture on the overall length of the wiring harness. Additionally, it facilitates the derivation of requirements for the introduced ZC, such as the number of loads to be supplied within each zone, the required supply power, and the load capacities to be managed during switch-on operations.

The number and size of the zones are predefined for the three vehicles, as illustrated in Figure 1. This limitation arises from the need to adapt the zone borders to the vehicle's boundary conditions and ensure appropriate placement of the ZCs. The zones are designed to allow an even distribution of loads per zone. For instance, the boundary between the front zone(s) in the engine compartment and the cabin is always located near the firewall. This is why a four-zone division into vehicle corner quarters, as often depicted in schematics for zonal architectures, is impractical, as many cables would traverse the firewall (e.g., [7], [17], [18]).

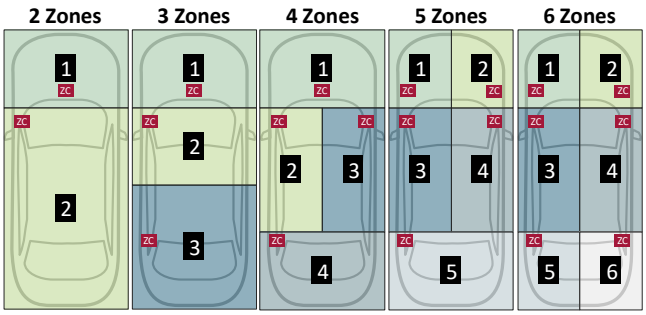

Figure 1: Different number of possible zone configurations.

The position of the ZCs is generally based on the location of the former fuse boxes, where feasible, to ensure available installation space and so varies a little between the analyzed vehicles. The usual positions are shown in Figure 1 and explained in the following. In the two-zone configuration, one ZC is placed near the low-voltage LV-battery in the engine compartment, while the second ZC is located below the A-pillar on the drivers side. For the three-zone variant, the boundary between zones 1 and 2 remains the same, and a new boundary is introduced to divide zones 2 and 3 behind the front seat row. The third ZC is positioned at the rear of the vehicle, near the trunk, where some larger vehicles also place fuse boxes and where the wiring harness typically splits.

In the four-zone configuration, the zone in the engine compartment remains unchanged, while the passenger cabin is split into left and right zones, while the fourth zone covers the trunk. The reason for dividing zones 2 and 3 into two smaller zones is the concentration of many loads in the driver and passenger seat regions. The ZCs are positioned below the left and right A-pillars for zones 2 and 3, with the ZC in the rear remains at the same location as in the three-zone setup. For the five-zone and six-zone configurations, the approach is similar (see Figure 1).

Only few OEMs currently have implement ZCs, those that do tend to follow a similar placement strategy. For example, the Tesla Model 3 uses two ZCs, one on each side below the A-pillar [14], and the Rivian Gen 2 places one ZC at the side in the rear of the vehicle [19].

In contrast a second option is to have a higher-level power distribution unit (PDU). The PDU supplies the ZCs, and additional loads can be selected for direct supply by the PDU. This is particularly useful for high-power loads such as steering and braking, as it minimizes voltage drops in the wiring harness and avoids transferring high power through the ZC. Other options include using the direct PDU supply for safety-critical loads or loads requiring key-off supply during parking mode. If the ‘higher-level PDU’ option is selected, the wires leading from the PDU to the ZCs are also included and their parameters are estimated.

3 Results & Discussion

In the following section the results are shown and discussed. Section 3.1 covers selected results of the measurement campaign, whereas section 3.2 demonstrates the usefulness of the zonal architecture tool.

3.1. Measurements

3.1.1 Wiring harness

In the measurement campaign data on the overall power distribution wiring harness was collected. For the vehicles from the B-, C-, and J-segment, the measured lengths were 213 meters, 339 meters, and 583 meters, respectively, which are notably shorter when compared to the values typically reported in the automotive industry. For the Audi E5 model of the PPE platform from the Volkswagen group, for example, the manufacturer specifies a total length of the wiring harness of around 3.6 kilometers [20], [21]. The reason for this deviation is that only the power distributing wires starting at a fuse boxes were analyzed, as described in Section 2.1, and not the communication wires, nor the supply lines which might follow downstream in some cases after an ECU. This highlights the size and complexity of the communication part of the wiring harness, which, combined with the power distribution part which was analyzed here, constitutes the overall wiring harness. Other researchers attempted to investigated the impact of a zonal architecture on the communication wiring harness with a different number of zones and developed an empirical equation to calculate the wiring harness length. However, with calculated total lengths of 50 to 250 meters excluding zonal segmentation, there appears to be a significant underestimation of the communication wiring harness, indicating potentially even higher benefits of a zonal architecture than it was indicated there [10]. The results of Maier et al. also oppose the study carried out here, as a total length of the wiring harness of 500 m was determined there, with an even distribution between communication and power supply [12]. At this point, it should be noted that the study by Maier et al. was primarily aimed at optimizing the number of zone controllers and not at measurement-based system-wide accuracy.

The analyzed wiring harness data also enabled weight calculations. For the J-segment-vehicle, the analyzed power distribution harness weighed approximately 18 kg, which, similar to its length, represents only a fraction of the total harness weight, estimated at approximately 59 kg for the Audi E5 [20], [21]. This weight discrepancy can be attributed not only to the absence of the communication wiring harness but also to the exclusion of the weight of plugs, connectors, and other ancillary components, which according to literature cause up to 50 % of the wiring harness weight [22].

As described in section 2.1, a wire length factor was calculated that represents the ratio between the actual wire length following its installation path and the geometric distance between a load and its respective supply point at the fuse box. For all three analyzed vehicles, this factor averages to a value of about 2.6. Although the ratio is not constant and decreases with increasing geometric distance, this average value can be used for initial estimates, as they are needed for the developed tool for the study of ZA configurations.

3.1.2 Load Measurements

In addition to the wiring harness, the LV-loads were examined. The total installed fuse values amount to 1497.5 A, 2297.5 A, 3885 A for the B-, C-, and J-segment-vehicles. These values, combined with their distribution function on specific values provide an initial estimation of the required electronic fuses necessary for a zonal architecture. The measured data can offer more helpful insights: the recorded maximum currents totaled 720 A for the B-segment, 826 A for the C-segment, and 968 A for the J-segment-vehicle. Discrepancies between fuse ratings and measured currents are attributed to multiple factors, including fuse cascading—where a single load current is protected at multiple cascading fuse boxes—gaps in the measurement campaign, and the fact that fuse values are typically rated for the wires they protect rather than the loads they supply. The maximum current is the sum of all peaks that recorded during the measurements. This includes DC motor inrush currents or current peaks that occur when capacities need to be charged. To better understand continuous load demands, maximum constant currents were analyzed, as detailed in Section 2.1. These currents totaled 316 A, 276 A, and 381 A for the B-, C-, and J-segment-vehicles, respectively. Notably, the higher value for the B-segment-vehicle is the result of the fact that the cabin heater is supplied by LV rather than by HV, which is a much more common practice.

Figures 2d–f illustrate the spatial distribution of maximum constant currents within the vehicles. In all cases, significant hot spots of power consumption can be found around the engine compartment. However, the J-segment-vehicle displays a more even distribution of current consumption throughout the vehicle, reflecting its extensive use of additional equipment e.g. for comfort functions frequently found in premium vehicles. This may indicate that more zones may be useful for this vehicle, to supply the additional equipment distributed throughout the vehicle body than the other two. The load maps help to determine the appropriate number of zones for each vehicle and can suggest optimal zone segmentations in relation to the proximity of the loads to be supplied.

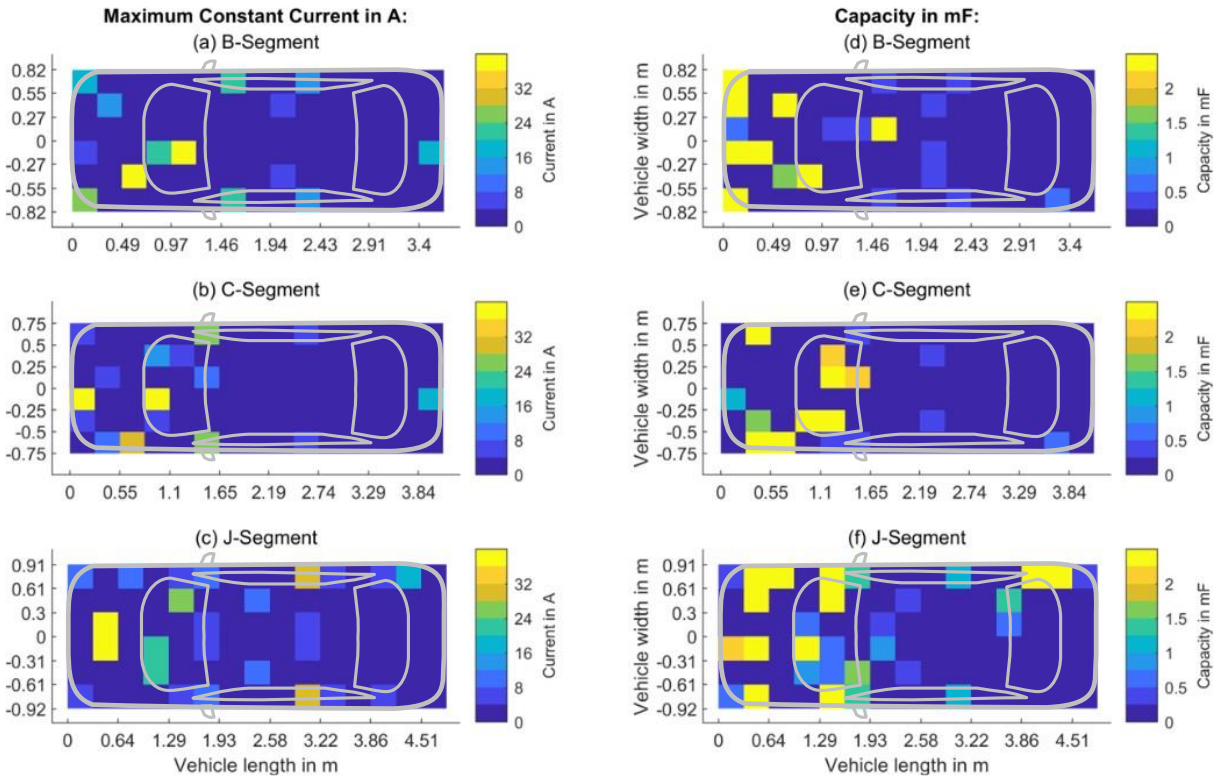

Figure 2: 2D map of maximum constant currents (a-c) and of capacities (d-f) of the different vehicles.

Figures 2a–c show the input capacitances measured on the various components of the LV power net. There is a pronounced concentration toward the vehicle's front. However, like for the maximum constant currents, the J-segment-vehicle exhibits a more even distribution of capacitances throughout the vehicle. The total capacitance within the LV power net sums up to 46 mF for the B-segment, 37 mF for the C-segment, and 68 mF for the J-segment-vehicle. The measured range of total capacities matches with the values found by Kull et al. who determined a total capacitance of 43 mF for an unspecified vehicle [15]. These input capacitances are particularly important in zonal architectures, where, unlike traditional power net configurations, individual loads can be switched on and off by using electronic switches in the ZC. In conventional power nets that use fuses and a limited number of relays, loads are switched according to terminal definitions, such as clamp 15 for those required in the ignition-on state. Most of these loads, along with their input capacitances, are continuously connected and charged to the battery voltage of approximately 12 V, even when the vehicle is idle.

In contrast, a power net based on a zonal architecture employing electronic fuses allows for the selective switching of individual loads. This means, for example, that in parking mode all loads that are not required can be switched off individually to avoid idle currents. However, this switching of loads with substantial input capacitances can lead to inrush current peaks, which must be properly managed. Advanced control algorithms can mitigate these peaks by regulating the linear range of the semiconductor switches of the electronic fuses [23]. Understanding the distribution of input capacitances, as depicted in Figures 2d–f, is crucial for determining where within the ZC such a functionality is needed and appropriate electronic fuse types must be chosen.

More details and results of the measurement campaign can be found in an earlier publication [16].

3.2 Zone Analysis

3.2.1 General Analysis

The measurement results provided the foundation for developing the zonal architecture tool. Figure 3 shows exemplary results that illustrate the spatial distribution of loads in an assumed zonal configuration in their position within the respective vehicle. Figure 3a depicts the 3-zone variant for the B-segment-vehicle, Figure 3b the 4-zone variant for the C-segment-vehicle, and Figure 3c the 5-zone variant for the J-segment-vehicle. The square symbols indicate the positions of the ZCs, and the circles indicate the positions of individual loads, with colors indicating their allocation to specific zones. As mentioned in the description from Figure 2, a significant number of loads is concentrated in the engine compartment across all types of vehicles. In case of the J-segment-vehicle (see Figure 3c), more loads are distributed throughout the entire vehicle.

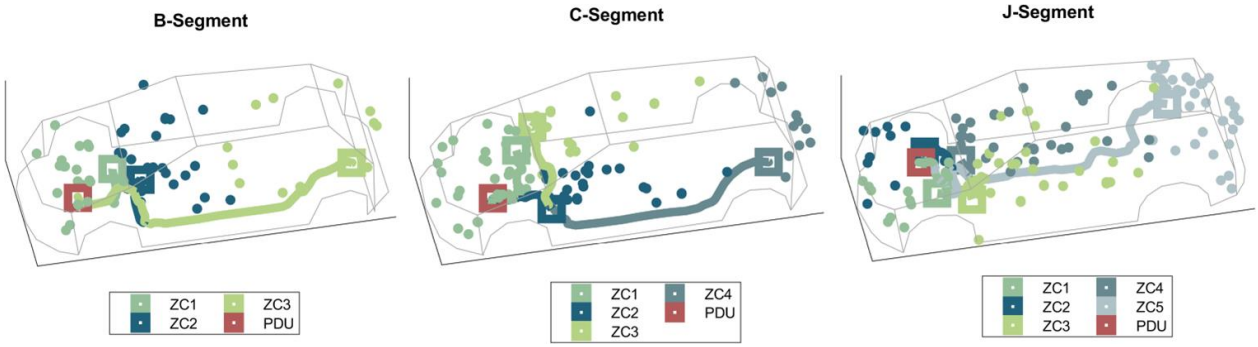

Figure 3: Re-distribution of the loads in the different vehicle classes into a variant number of zones. The colors of the circles indicate the zonal allocation.

Figure 4 displays the impact of the selected zonal distribution on potential ZCs. Figures 4a–c shows the number of loads connected to each ZC, and Figures 4d–f the summed up resulting maximum constant currents for each ZC. The variants depicted in Figure 3 are highlighted in red. One zone segmentation strategy might be to have ZCs that are as similar as possible to create identical structures to match a common parts strategy. One can observe that this is the case for the 3-zone configuration for the B-segment-vehicle, resulting in an almost equal distribution of number of loads and sum of maximum constant currents between the ZCs. For the C-segment-vehicle, introducing a fourth zone does not substantially improve an even load distribution compared to the 3-zone configuration. In this configuration, further dividing the engine compartment could have been more beneficial for an even current and load distribution. For the J-segment-vehicle, the 4-zone

configuration provides the most balanced distribution of loads per zone. In terms of maximum constant currents, a more even distribution is achieved with the 5-zone configuration. Unlike the C-segment-vehicle, which does not seem to benefit from the additional fourth zone, the J-segment-vehicle does. This can be attributed to the fact that the loads are distributed more evenly over the entire vehicle body. The analysis also reveals that the most powerful loads in the J-segment-vehicle are located in zones 1 and 2 within the engine compartment. For example, if the current is divided by the number of loads per zone, it can be seen that in the 5-zone configuration, zone 1 has an average maximum continuous current of 4.8 A, while the average current in zone 5, which is in the main line, is 0.5 A

These results are useful for identifying requirements for ZCs. The data can be used to select suitable electronic fuses capable of carrying the required currents, and initial estimates can also be made for a cooling concept. On the control side, the tool can help to identify which functions are required for a specific ZC. For example, zones ZC 3 and 4 in the 5-zone J-segment-vehicle require an electric window function with all the necessary additional features such as anti-pinch control and icing detection, while zone 5 requires various rear light functions.

In further analysis, the different vehicle segments in Figure 4 could be examined. From the perspective of a common parts strategy, it might be desirable to design zones in such a way that similar ZCs can be used in vehicles from different segments. Looking at the ZC1 in the B-segment, it can be seen that both the currents and loads per ZC are similar to the ZC1 in the 3- or 4-zone configuration of a J-segment vehicle. Considering that in both cases the engine compartment is supplied with power and therefore similar functions are required, an OEM could try to develop them as common parts. However, it is important to note that load configurations are highly customized and highly dependent on the OEM's specific vehicle design and configuration. By aligning zones to support a common parts strategy, there might be an opportunity to improve the scalability and cost efficiency of ZC deployment across different vehicle models.

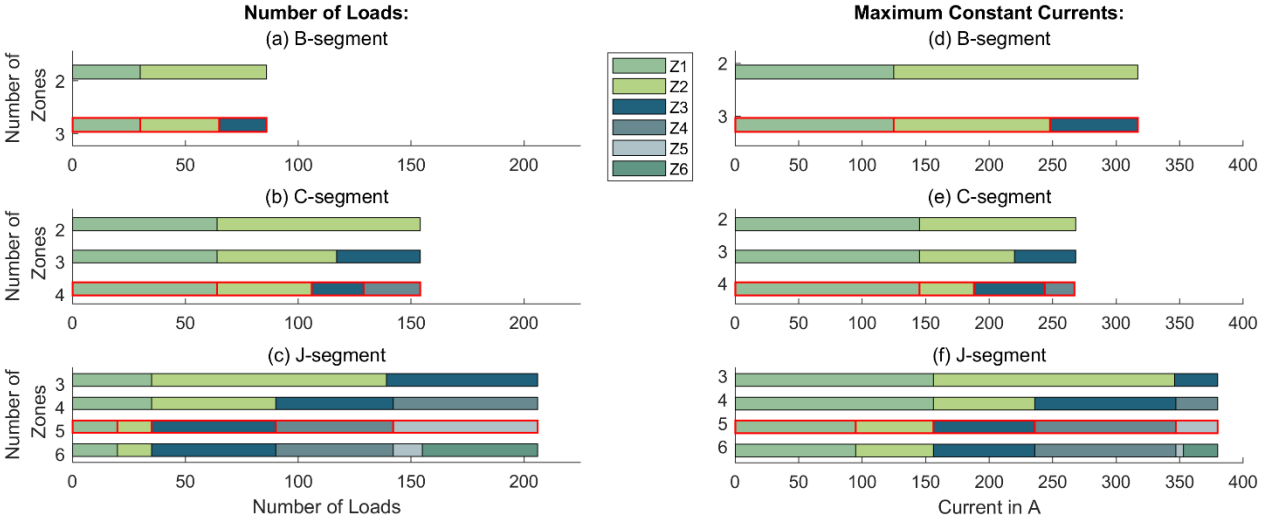

Figure 4: Distribution of loads and currents to the different ZCs for the different configurations. The configurations shown in Figure 3 are highlighted in red.

The allocation of loads to zones also impacts the wiring harness. Based on average factors (see Section 2.1), new wire lengths for the zonal configurations were determined. This allows for a comparison of different variants with a varying number of zones in terms of wiring harness reduction, as shown in Figure 5. A reduction of the length of the analyzed wires is evident for all variants, except the 2-zone C-segment-vehicle, which would be a reduction of supply points (the original vehicle has three fuse boxes). Implementing a 3-zone architecture would reduce the analyzed wire length by approximately 40% for the B-segment, 26% for the C-segment, and 30% for the J-segment-vehicle. The significant decrease in wire lengths in the J-segment-vehicle from the original configuration to the 3-zone variant is the result of the close proximity of ZC1 to the engine compartment loads. In the original vehicle, only the high-power loads were supplied via the engine compartment fuse box, while most other loads were connected to a large fuse box in the passenger compartment. Since a high number of loads is located in the engine compartment, the total wire length is reduced considerably. The additional, only slight reduction in wiring harness length with increasing number of zones is due to the fact that the original vehicle already had five distribution boxes, so that many consumers

could already be supplied from a nearby fuse box.

The calculated lengths are based on initial assumptions for zonal boundaries and the placement of ZCs as described in Section 2.2, which both leave space for additional optimizations. By optimizing the positioning of the ZCs within their respective zones, such as in the 6-zone configuration for the J-segment-vehicle, the length of the considered harness could be reduced by up to 53% compared to the original wiring, simply by placing the ZC in the center of all the loads to be powered. This optimization was performed without considering boundary conditions for the ZCs, such as available installation space, and aimed to highlight the tool's potential which can be par in future optimization. In future steps, the boundaries of zone could also be optimized to improve the wiring harness, and 3D boundaries could be considered to better adapt to constraints in vehicle design, such as grouping all loads within the vehicle roof into a single zone.

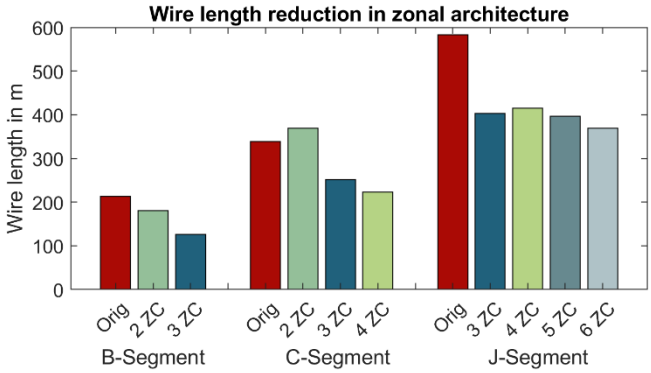

Figure 5: Potential wire length reduction for the different analysed vehicles.

Overall, the extent of wiring harness length reduction aligns with the findings of Park et al., who predict a reduction by approximately 30% when transitioning from a domain architecture to a 3-zone architecture, even though they use a completely different method for calculating wire lengths[10]. In contrast, Maier et al. report a reduction in harness weight but not in length as the number of zones increases [12].

3.2.2 Architecture Optimization

There are numerous possibilities for optimization in zonal architecture configurations. One approach is to focus on optimizing the architecture regarding the supply of safety-critical loads. Where an LV load is performing a safety-related function, the safety requirements usually extend to the power supply system and consequently to the ZC, depending on the safe state of the function. This in turn can result in extended safety requirements not only for the supplying electronic fuse, but also for all other output switches of the ZC, which inherit the safety requirements and ensure safe disconnect functionality to ensure freedom from interference with other loads. Moreover, the entire ZC development process must adhere to ISO 26262 standards [24]. One strategy to optimize a ZA could be to concentrate the supply of all safety-critical loads within one or a few ZCs, which would then be developed according to ISO 26262, thereby relieving the majority of ZCs from safety-related requirements.

To test this concept, the database was enriched with safety information. The hazard and risk analysis (HARA) that leads to an Automotive Safety Integrity Level (ASIL) classification according to ISO26262 is a dynamic process. Different HARA teams may arrive at different results, e.g. by taking into account different local conditions like speed limits and road conditions. Publicly accessible data sources are limited, as companies often hesitate to expose their results to external scrutiny, given the time-consuming and confidential nature of the analysis. For this study, data from [25]–[29] was used, encompassing safety requirements for components such as the low beam, brake lights, and radar sensors. Loads identified as safety-critical are marked with red circles in Figure 6 for the 6-zone variant of the J-segment-vehicle. The graphic illustrates that the considered safety loads are distributed across the entire vehicle. All safety-relevant loads were connected to the two ZCs centrally located in the vehicle to consolidate safety requirements on these devices. Consequently, ZCs 3 and 4 take over an additional safety-domain-controller function, thereby reducing safety requirements for the remaining ZCs.

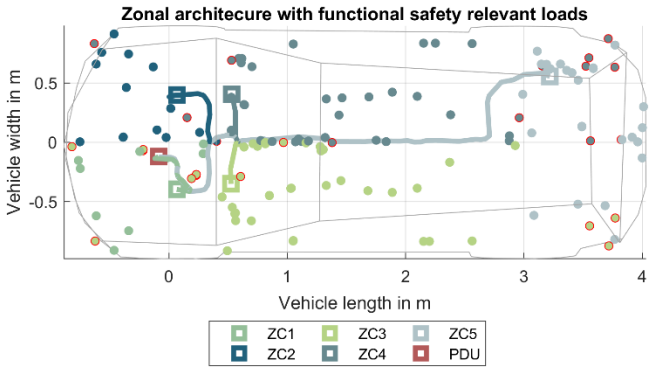

Figure 6: Optimized zonal architecture with safety relevant loads (highlighted red) concentrated in zone 3 and 4.

In return, the wiring harness length increases from 369 meters to 460 meters compared to the 6-zone variant without consolidating safety loads. However, by optimizing the positions of the ZCs, as previously described, it was possible to further reduce the wiring length to 364 meters.

Another optimization approach involves shifting all high-power loads to a higher-level PDU. This strategy would reduce the current that needs to pass through the ZCs, potentially improving voltage stability within the zones and decreasing the cooling requirements for the ZCs. Yet another option is to evaluate all loads for key-off supply requirements and concentrate the corresponding loads into one or few zones. The respective ZCs would then fulfill the required key-off functionality, which is currently managed by multiple individual ECUs and supply key-off relevant loads (e.g. key-less go antennas). This method, similar to the approach discussed for safety loads, could simplify vehicle operation. Most of the system, including the majority of ZCs, could be turned off when the vehicle is parked, with only the ZCs responsible for key-off functionality remaining active. Of course, there are many other system requirements besides pure power supply that have not been considered in these suggestions, which are intended as a stimulus for thought.

3.2.3 Implications on System Level

When implementing a zonal architecture, it is essential to consider the transformation of the entire power net architecture. Components are grouped into new electrical "islands" or zones, with lower wire resistances and inductances between them. In the 6-zone J-segment vehicle, trunk components like the tail light and rear window wiper are now supplied by a local ZC, reducing wire length from 7.5 meters to 2 meters, resulting in a decreased wire resistance and inductance. This in turn causes entirely new interactions between the individual loads in a zone. For example, dynamic under- and over-voltages caused by wire impedance in combination with load currents will change and possibly spread easily between all the loads in a zone due to the lower impedance in between. Moreover, the input capacities of the loads, which are required to stabilize the voltage and to comply with LV124 [30] will react differently in the new configuration.

System simulations are a powerful tool for analyzing the new system behavior in a zonal architecture. They can, for example, support the evaluation of the over-voltages and under-voltages occurring at the loads and in the various ZCs. Switching processes can be analyzed and suitable measures, such as pre-charging algorithms or a controlled disconnection, can be prepared and tested.

All parts of the presented analysis are based on the conducted measurements and could be executed in a similar way if suitable test vehicles and 3D analyze tools are available. For an OEMs, who naturally has full access to all the required data on the structure of all its loads and their properties, an even more detailed analysis is possible.

4 Summary & Outlook

This study outlines an innovative approach to designing zonal configurations of the LV loads and the wiring harness for BEVs using extensive, real-world measurements. By compiling detailed wiring harness measurements with LV-load data, a comprehensive database has been built as a basis for a zonal LV architecture tool. This tool facilitates an early-on analysis of how a chosen zone configuration affects new potential ZCs and the wiring harness. Conducting this kind of initial system level analysis is advisable when transitioning to a zonal architecture, as it can help to maximize the potential benefits and mitigates the risk of investing time and effort in less beneficial solutions.

Early consideration of factors such as the supply of safety-critical or key-off loads and the of potential ZC performance requirements is crucial. This foresight extends to ZC placement decisions, determining requirements such as cooling needs or specific development processes necessary for safety compliance. The allocation of loads into zone significantly influences the wiring harness; for instance, a 3-zone architecture can lead to a reduction of the length of the considered wires of 26% to 40%. The smaller sub-units of the harness also offer advantages for the manufacturing process and for vehicle integration.

Due to the complete redesign of the power supply net, the physical behavior of the newly formed zonal power supply architecture must also be considered. The data and results generated through this study serves as a foundation for simulating the physical behavior of the system, ensuring that any physical interactions and potential issues can be anticipated and addressed.

Overall, this research contributes to the advancement of next-generation EVs, aiming to make them safer, more scalable, and easier to manufacture.

5 References

[1] C. Werwitzke, “Rivian und Volkswagen gründen Software-Joint-Venture,” *electrive.net*, 2024, [Online]. Available: https://www.electrive.net/2024/11/13/rivian-und-volkswagen-gruenden-software-joint-venture

[2] P. Zollino, C. Hauss, J. Kulawik, M. Hoffmann, Volkswagen Group, and Rivian, “Volkswagen Group und Rivian kündigen Pläne für Joint Venture zur Schaffung einer branchenführenden Fahrzeugsoftware-technologie und für eine strategische Investition durch Volkswagen an,” 2024. [Online]. Available: https://www.volkswagen-group.com/de/partnerschaft-zwischen-volkswagen-group-und-rivian-18383

[3] A. Antlitz, “12.11.2024 - Volkswagen Group \& Rivian Announce Inception of Joint Venture – Präsentation von Dr. Arno Antlitz, CFO/COO Volkswagen Group,” 2024. [Online]. Available: https://www.volkswagen-group.com/de/partnerschaft-zwischen-volkswagen-group-und-rivian-18383

[4] S. Munro and Munro Live, “Inside Rivian’s Electrical Hardware Lab with Vidya Rajagopalan,” Youtube, 2025. [Online]. Available: https://www.youtube.com/watch?v=zlpTQePnfNw

[5] Tesla Inc., “2023 Investor Day | Tesla - YouTube,” 2023. Accessed: Apr. 07, 2025. [Online]. Available: https://www.youtube.com/watch?v=Hl1zEzVUV7w

[6] C. Park and S. Park, “Performance Evaluation of Zone-Based In-Vehicle Network Architecture for Autonomous Vehicles,” *Sensors*, vol. 23, no. 2, 2023, doi: 10.3390/s23020669.

[7] O. Burkacky, J. Deichmann, M. Kellner, F. Steiner, J. Werra, and McKinsey \& Company, “Getting ready for next-generation E/E architecture with zonal compute - Whitepaper,” 2023. [Online]. Available: https://www.mckinsey.com/industries/semiconductors/our-insights/getting-ready-for-next-generation-ee-architecture-with-zonal-compute#/

[8] F. Daniel, A. Eppler, T. Schwarz, M. Bauer, and Roland Berger, “THE WIRING HARNESS SEGMENT – KEEPING UP OR FALLING BEHIND ? - Whitepaper,” 2022. [Online]. Available: https://content.rolandberger.com/hubfs/Harness_Market_Study_2022.pdf?utm_campaign=22-0023_European-pe-outlook&utm_medium=email&_hsenc=p2ANqtz-_ItmK7eee3Tmdu_8eABvOx2RYVELfYNUuIMW8-giU53Shbkh7pep4NMKazuBXF6DV7Fs4nv3xcM70hiGcujsrvlFTjjrM55Wgr2nKW1-e4CmtEhsk

[9] BMW AG, “BMW Group Investor \& analyst days 2024 - Whitepaper,” Munich, 2024.

[10] C. Park, C. Cui, and S. Park, “Analysis of E2E Delay and Wiring Harness in In-Vehicle Network with Zonal Architecture,” *Sensors*, vol. 24, no. 10, 2024, doi: 10.3390/s24103248.

[11] H. Jang, C. Park, S. Goh, and S. Park, “Design of a Hybrid In-Vehicle Network Architecture Combining Zonal and Domain Architectures for Future Vehicles,” *Proc. 2023 IEEE 6th Int. Conf. Knowl. Innov. Invent. ICKII 2023*, pp. 33–37, 2023, doi: 10.1109/ICKII58656.2023.10332574.

[12] J. Maier and H. C. Reuss, “Design of Zonal E/E Architectures in Vehicles Using a Coupled Approach of k-Means Clustering and Dijkstra’s Algorithm,” *Energies*, vol. 16, no. 19, 2023, doi: 10.3390/en16196884.

[13] V. Bandur, G. Selim, V. Pantelic, and M. Lawford, “Making the Case for Centralized Automotive E/E Architectures,” *IEEE Trans. Veh. Technol.*, vol. 70, no. 2, pp. 1230–1245, 2021, doi: 10.1109/TVT.2021.3054934.

[14] A2MAC1 Group, “A2MAC1.” [Online]. Available: www.a2mac1.com

[15] M. Kull, K. Feser, and U. Reinhardt, “Measurements and simulations of transient switching phenomena in modern passenger cars,” *SAE Tech. Pap.*, vol. 113, no. 2004, pp. 221–225, 2004, doi: 10.4271/2004-01-1704.

[16] S. Jagfeld, T. Schlautmann, R. Weldle, A. Fill, and K. P. Birke, “Creating an Extensive Parameter Database for Automotive 12 V Power Net Simulations : Insights from Vehicle Measurements in State-of-the-Art Battery Electric Vehicles (BEVs),” *To be Publ.*, 2025.

[17] A. T. Vemuri and Texas Instruments, “Processing the Advantages of Zone Architecture in Automotive - Whitepaper,” 2023. [Online]. Available: https://www.ti.com/document-viewer/lit/html/SSZT211

[18] M. Bornemann and Aptiv, “Zone Controllers Build Bridge to Tomorrow ’ s Technology - Whitepaper,” 2021. [Online]. Available: https://www.aptiv.com/docs/default-source/white-papers/2021_aptiv_whitepaper_zonecontroller.pdf

[19] Rivian, “Rivian Investor Day Forward-Looking Statements -Whitepaper,” 2024. [Online]. Available: https://downloads.rivian.com/2md5qhoeajym/29B1jJmErhGosTcyaS5Lci/4c04aba25a22778e3a9516cedaac2ddd/062724_Rivian_InvestorDay.pdf

[20] M. Frauenhofer, “Bordnetz im PPE,” in *Kooperationsforum Bordnetze*, Kooperationsforum Bordnetze, 2024.

[21] U. Hoff, D. Scott, and Siemens AG, “Automotive Trends Creative New Challenge for Wiring Harness Development - Whitepaper,” 2019. [Online]. Available: https://resources.sw.siemens.com/en-US/white-paper-automotive-wiring-harness

[22] M. Diebig, “Entwicklung einer Methodik zur simulationsbasierten Dimensionierung von Kfz-Bordnetzen,” Technische Universität Dortmund, 2016.

[23] K. Ludwig and F. Rifai, “POWER DISTRIBUTION IN MODERN VEHICLE ARCHITECTURES,” in *Elektrik, Elektronik in Hybrid- und Elektrofahrzeugen 2024*, Essen, Germany: Haus der Technik, 2024.

[24] ISO, “ISO 26262-4 Road vehicles — Functional safety — Part 4: Product development at the system level,” p. 13, 2018.

[25] HELLA, “Safety is no coincidence | HELLA | HELLA.” Accessed: Feb. 19, 2025. [Online]. Available: https://www.hella.com/soe/en/News/Safety-is-no-coincidence-5391/

[26] Synopsis, “What is ASIL (Automotive Safety Integrity Level)? – Overview | Synopsys.” Accessed: Feb. 19, 2025. [Online]. Available: https://www.synopsys.com/glossary/what-is-asil.html

[27] Jama Software, “Meeting Regulatory Compliance and Industry Standards - Jama Software.” Accessed: Feb. 19, 2025. [Online]. Available: https://www.jamasoftware.com/requirements-management-guide/automotive-engineering/guide-to-automotive-safety-integrity-levels-asil/

[28] STW Mobile Machines, “Functional safety at the next level | STW.” Accessed: Feb. 19, 2025. [Online]. Available: https://www.stw-mobile-machines.com/en/news/detail/functional-safety-at-the-next-level/

[29] Florian Rohde and Ivan Celanovic, “ASIL for Electric Vehicles and EV Powertrains - Typhoon HIL.” Accessed: Feb. 19, 2025. [Online]. Available: https://www.typhoon-hil.com/blog/asil-electric-vehicle-powertrains/

[30] German Automotive Manufactures, “LV124: Test procedures for electrical and electronic components in vehicles.,” 2013

6 Presenter Biography

Sebastian Jagfeld is an PhD candidate within the Technology & Innovation Department of Schaeffler AG in Regensburg, Germany. He is currently researching in the field of future automotive power supply nets through simulation and measurement. He graduated from the University of Stuttgart with a Master of Science in Energy Engineering in 2022. In 2018, he received his bachelor’s degree in mechanical engineering from FAU University Erlangen-Nuremberg.